



HAL
open science

Generation of weather data for the assessment of building performances under future heatwave conditions

Adrien Toesca, Damien David, Kévyne Johannes, Michel Lussault

► To cite this version:

Adrien Toesca, Damien David, Kévyne Johannes, Michel Lussault. Generation of weather data for the assessment of building performances under future heatwave conditions. *Building and Environment*, 2023, 242, pp.110491. 10.1016/j.buildenv.2023.110491 . hal-04409164

HAL Id: hal-04409164

<https://hal.science/hal-04409164v1>

Submitted on 22 Jan 2024

HAL is a multi-disciplinary open access archive for the deposit and dissemination of scientific research documents, whether they are published or not. The documents may come from teaching and research institutions in France or abroad, or from public or private research centers.

L'archive ouverte pluridisciplinaire **HAL**, est destinée au dépôt et à la diffusion de documents scientifiques de niveau recherche, publiés ou non, émanant des établissements d'enseignement et de recherche français ou étrangers, des laboratoires publics ou privés.

Generation of weather data for the assessment of building performances under future heatwave conditions

Adrien Toesca^a, Damien David^{a,1*}, Kévy Johanes^a, Michel Lussault^b

5

^a Univ Lyon, INSA Lyon, CNRS, CETHIL, UMR5008, 69621 Villeurbanne, France

^b University of Lyon, UMR 5600 EVS, Lyon, France

Abstract

10 Heatwave weather files are needed to assess building performance under future
heatwaves. This paper presents a methodology for producing a minimum set of
heatwave weather files, which should be representative of the diversity of heatwaves
expected in a location of interest. It is a four-step methodology. Weather projections
are first collected from the CORDEX project database. Then, heatwaves are identified
15 in the weather data. A list of independent and significant indicators is constructed to

* This is to indicate the corresponding author.

Email address: damien.david@insa-lyon.fr

Address: Bâtiment Sadi-Carnot, 9, rue de la Physique, Campus LyonTech La Doua,
69621-Villeurbanne cedex, France

Abbreviations

BPI	Building Performance Indicator
CORDEX	COordinate Regional Downscaling Experiment
CMA	Correlation Matrix Analysis
DMT	Daily Mean Temperature
EHF	Excess Heat Factor
GCM	Global Circulation Model
HWMI	HeatWave Magnitude Index
IBM	Indicator Biometeorological
IWEC	International Weather for Energy Calculation
PC	Principal Component
PCA	Principal Component Analysis
RCM	Regional Circulation Model
RCP	Representative Concentration Pathway

characterise the heatwaves. Samples of heatwaves are finally selected based on the list of indicators. The methodology was tested for the location of the Lyon-Saint Exupery Airport. A total of 2229 heatwaves were identified within 1260 years of weather projections. The heatwaves showed a high degree of diversity in terms of weather characteristics. The sampling process selected only 8 representative heatwaves. This number is sufficiently reduced to consider using the reduced set of heatwave weather files for assessing building performance.

Keywords: Heatwaves, global warming, building simulations, weather data

1. Introduction

During the next decades, it is highly probable that a majority of the buildings on earth will experience several heatwaves. Additionally, the heatwaves to which each building may be exposed are likely to have different characteristics. Some of them will last longer, some of them will have higher temperatures, etc. The wide variety of heatwaves to which a building could potentially be exposed can be attributed to the stochastic nature of extreme meteorological phenomena. It is also due to the uncertainty in the evolution of the climate, which may be attributed to both the uncertainty in the evolution of greenhouse gas emissions and the limitations of the models used to predict future climate evolution [1]. Considering the diversity of the heatwaves that a building may have to face during the next decades, a question arises: is it relevant to assess the performance of the building during future heatwaves by simulating the building thermal behaviour under the conditions of a unique heatwave? To the authors' point of view, most of the time it is not relevant. Instead, a set of heatwave weather files would be needed to assess the building performance, with the heatwaves being representative of the diversity of the future probable heatwaves at the building location.

Some authors have developed and tested different methods to constitute such a set of heatwave weather files. [2] studied the thermal performance of buildings equipped with phase change material panels under heatwave conditions in Melbourne. They used the weather data of the 2009 heatwave as a base file. To consider the impacts of climate

45 change, they constructed heatwave weather data for 2030 and 2050 by increasing the
air temperature of the 2009 heatwave by 1 °C and 1.5 °C, respectively. They did not
modify the other weather variables. This method does not produce heatwave datasets
that are representative of the diversity of future heatwaves because the weather data are
too similar.

50 [3] studied resilient retrofitting strategies of buildings under future heatwave
conditions. They used three heatwave weather files. Those weather files were produced
by selecting the hottest summer week of the representative International Weather for
Energy Calculation (IWEC) weather data of three Mediterranean cities located in
different climate zones. The method relies on the assumption that the time variability
55 of future heatwaves could be similar to the spatial variability of current heatwaves.

[4] developed a method for defining reference summer weather year (RSWY)
weather files from historical weather data over a period of 31 years. The method defines
a heatwave as an event during which the t-Standard Effective Temperature (t-SET)
comfort index, computed with weather data, remains over an arbitrary threshold for
several consecutive days. The authors calculate three indicators for each heatwave: the
60 duration, the severity (surface between the t-SET time evolution over the threshold) and
the intensity (ratio between severity and duration). The RSWYs are the second most
extreme years (over the 31 historical years) in terms of heatwave duration, intensity or
severity. There can therefore be 3 RSWYs for a given period and location. It is also
65 possible that the same year is the second most extreme on all 3 indicators. To the present
authors' knowledge, the method has only been applied to historical weather data.

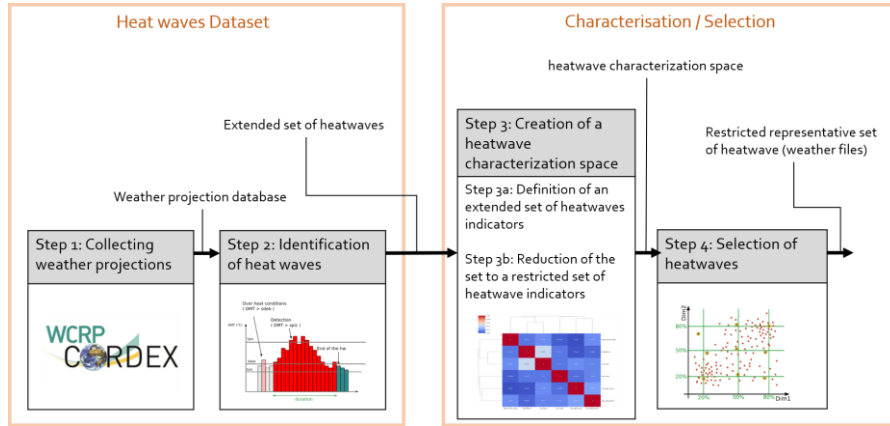
[5] built Future Typical Weather Year (FTWY) weather files from weather
projection data for the location of Nantes, France. The authors compared the FTWYs
obtained with weather data produced by three different climate projection models to the
70 weather data of 2003, during which a deadly heatwave occurred in France. They
observed that the heatwaves contained in their future typical weather data years were
less extreme than the 2003 heatwave. This may be true for the heatwaves contained in
typical weather files, but this may not be true for more extreme future heatwaves. In the
authors' view, extreme weather files should only be compared with extreme files and
75 not with typical weather files.

None of the methodologies mentioned here can be used to produce a representative set of heatwave weather files for building assessment. The methods for producing representative meteorological years do not focus enough on the heatwave characteristics. Most of the methodologies are only based on an analysis of the air temperature evolution, but a building's thermal behaviour strongly depends on other weather variables, such as solar radiation, wind speed, or sky temperature. Finally, none of the methodologies are able to assess the representativeness of the set of heatwave weather files regarding the possible diversity of future heatwave characteristics.

The present paper describes a methodology that intends to construct a minimum representative set of heatwave weather files for building assessment. It is a four-step methodology. An overview of the methodology is proposed in the first section. A detailed description of each step is provided in the following sections. The description of the methodology is illustrated by an application for the location of the Lyon-Saint Exupéry Airport.

90 **2. Methodology overview**

Figure 1 summarizes the overall methodology. The first step consists of collecting weather projections for the locality of interest. Here, the term "weather projection" refers to a long-term weather prediction. The second step consists of identifying heatwaves in the weather projections. This data produces the extended heatwave dataset. The third and fourth steps intend to sample the extended heatwave dataset. The third step consists of building a heatwave characterization space in which each heatwave is located according to its characteristics. The fourth step consists of selecting heatwaves in the characterization space.



100

Figure 1: Scheme of the methodology

For the purpose of this paper, the four-step methodology has been applied to the case study of the Lyon_Saint Exupéry Airport, France. Table 1 provides general information about the case study. The Lyon-Saint Exupery Airport is located in a rural area, 30 km away from the city of Lyon, France. The method is applied in rural areas and therefore does not consider urban heat island effects. Thus, the results of the method will not depend on assumptions about the evolution of cities, which will allow the set of heatwaves to be used later as a base to simulate the urban heat island effects during future heatwaves for different urbanisation.

105

Table 1: General information on the case study

Name	Latitude	Longitude	Altitude	Time Zone
Lyon-Saint Exupéry	45.7261 45° 43' 34" North	5.09083 5° 5' 27" East	250 m	UTC +1:00 (Europe/Paris) Summer time: UTC +2:00 Winter time: UTC +1:00

110

3. Detailed description of the methodology

3.1. Step 1: Collecting climate projection data

3.1.1. Objectives and method

The first step consists of collecting weather projections. Weather projections
115 produced with the morphing method are not suitable for the study of future heatwaves.
The morphing method produces weather variable time series whose average value and
amplitude are different. However, those time series evolve with a similar pattern,
regardless of the climate evolution scenario. The method does not allow us to consider
120 the variations in frequencies and time durations of extreme weather events such as
heatwaves [6]. In contrast, dynamical downscaling models are able to reproduce
random events. Weather projections that are produced with the dynamical downscaling
method are more suitable.

The COordinate Regional Downscaling Experiment (CORDEX) database contains
weather projection data produced with the dynamical downscaling method. In the
125 CORDEX database, each weather projection corresponds to one Representative
Concentration Pathway (RCP) scenario and one projection model. Each model is the
combination of a global circulation model (GCM), which produces climate projections,
and a regional circulation model (RCM) for the dynamical downscaling process. The
CORDEX database contains a great variety of climate projections. However, a large
130 number of climate projections cannot be exploited in the present context. The
projections must fulfil criteria to produce relevant weather data for building
simulations.

Building simulation weather files contain a fixed list of variables for which data must
be provided with an hourly timestep. There is no weather projection in the CORDEX
135 database that contains all the required variables. Moreover, the number of available
variables may vary greatly between the different weather projections. There are
techniques to compute missing weather variables, but to maximize the degree of
confidence in the resulting data, a minimum list of available variables has been
established. To be considered suitable, a CORDEX weather projection must contain
140 data for all the variables contained in the minimum list of required variables given in
Table 2. This list is a compromise between the list of commonly available variables in
the CORDEX database and the list of variables required in the building simulation
weather files. The present list contains three additional variables compared to the

145 minimum list of required variables proposed by Machard et al. (2020): the incident
 infrared radiation and the two components of the wind velocity, which are used to
 compute the wind direction. The variable names in Table 2 follow the CF (Climate and
 Forecast) standard. The technique from [1] is used to compute the missing weather
 variables.

150 Hourly data are not common in the CORDEX database. They are available on a
 three-hourly or longer time step. The CORDEX weather data must be interpolated to
 obtain hourly data. To minimize the degradation of the information due to interpolation,
 a maximum time step was fixed for each variable. The maximum timesteps are listed
 in the second column of Table 2. A CORDEX weather projection is suitable only if, for
 all the variables in Table 2, data are available at a timestep lower than or equal to the
 155 related maximum timestep.

The future heatwave weather data are intended to be used for the evaluation of the
 absolute building performances during future heatwaves, as opposed to a comparative
 evaluation with a reference building behaviour evaluated during a reference historical
 period. In that context, there is general agreement on the fact that bias-corrected weather
 data should be used [5]. In the CORDEX database, bias-corrected data are available
 160 only for 3 variables: the air temperature, the wind speed and the global solar irradiation.
 Only the weather projections for which bias-corrected data are available for those 3
 variables are considered suitable.

165 The first step of the methodology consists of identifying suitable weather projections
 according to the three criteria presented above, downloading the related weather data,
 computing the missing weather variables, and interpolating the data linearly to obtain
 the full list of data that is required in building performance simulation weather files.

Table 2: Minimum requirements for a CORDEX weather projection to be considered suitable

List of required variables	Maximum Timestep	Bias-correction availability
Dry air temperature [K]	3 hrs	Yes
Specific humidity [kg/kg]	3 hrs	-
Atmospheric pressure [Pa]	3 hrs	-
Cloud fraction [%]	3 hrs	-
Global horizontal radiation [W/m ²]	3 hrs	Yes
Wind speed [m/s]	3 hrs	Yes

Precipitation [kg/m ² /s]	3 hrs	-
Surface Downwelling Longwave Radiation [W/m ²]	3 hrs	-
Eastwards wind speed [m/s]	6 hrs	-
Northwards wind speed [m/s]	6 hrs	-

3.1.2. Application

170 Table 3 shows the result of the weather projection selection for the location of Lyon-St Exupery. The Lyon St-Exupery site is located in the EURO-CORDEX subdomain of the CORDEX project. The selection of weather projections (Table 3) is relevant for any location in this subdomain.

Fourteen weather projections were selected. They correspond to 2 RCP scenarios, 175 RCP4.5 and RCP8.5, and 7 different models. The 7 models are combinations of 5 distinct GCMs and 2 distinct RCMs. Each weather projection runs from 2007 until 2097. The whole weather projection dataset represents 1260 years of weather projection.

180 *Table 3: List of the weather projections collected from the CORDEX database. Crosses indicate data availability.*

GCM	RCM	Ensemble	rcp45	rcp85
CNRM-CERFACS-CNRM-CM5	RCA4	r1i1p1	X	X
ICHEC-EC-EARTH	RAMCO22E	r1i1p1	X	X
IPSL-IPSL-CM5A-MR	RCA4	r1i1p1	X	X
MOHC-HadGEM2-ES	RAMCO22E	r1i1p1	X	X
MOHC-HadGEM2-ES	RCA4	r1i1p1	X	X
MPI-M-MPI-ESM	RCA4	r1i1p1	X	X
ICHEC-EC-EARTH	RCA4	r12i1p1	X	X

3.2. Step 2: Identifying heatwaves

3.2.1. Objectives and method

185 The second step of the methodology consists of identifying heatwaves in the weather projections. There is no universal definition of a heatwave, but the literature frequently refers to four heatwave identification methods: the "Spic, Sdeb, Sint" method from [7], the "IBM" method from [8], the Excess Heat Factor ("EHF") method from [9] and the HeatWave Magnitude Index ("HWMI") method from [10].

To avoid inconsistencies in the heatwave dataset, a choice must be made between the four identification methods. It is not possible to base that choice on the description of the four identification mechanisms. Therefore, it was decided to perform heatwave identification with the four methods and to identify the most appropriate method from a comparison of the resulting heatwave datasets.

3.2.2. Application

Table 4 contains a statistical description of the four heatwave datasets for the location of Lyon-St Exupery. For each heatwave dataset, the first column contains the average number of identified heatwaves per year, the second column contains the average duration of the heatwaves, the third column contains the average value of the average temperatures during the heatwaves, and the fourth column contains the absolute number of identified heatwaves.

The “EHF” and “HWMI” methods identified a considerably larger number of heatwaves than the first two methods. Their identification criteria are less restrictive, with lower threshold values. As a result, the average temperature during a considerable part of the heatwaves is mild. However, health and discomfort issues might be expected during more extreme events. For this reason, those two methods were not chosen.

The distinction between the "Spic, Sdeb, Sint" method and the “IBM” method is more subtle. The two methods identified roughly the same number of heatwaves, and a deeper analysis of the datasets reveals that 90% of the heatwaves identified by the two methods correspond to the same extreme weather event: the same period of the same weather projection. The major difference between the 2 methods is the criterion used to locate the beginning and end of the heatwaves. This criterion is less restrictive for the "Spic, Sdeb, Sint" method in which the heatwaves start earlier and finish later. As a consequence, the heatwaves last for longer (8 days on average), with a lower average air temperature (2 °C on average). The "IBM" method only identifies the heart of heatwaves. Although those observations reveal some specificities of the two heatwave identification methods, they did not motivate the choice between the two methods.

Finally, the “IBM” method was chosen. The main reason for that choice is that the method is used by France’s Heat Health Watch Warning System to trigger heatwave alerts [8].

220 The second step of the methodology, applied to the Lyon St Exupery, resulted in the construction of a dataset containing 2229 heatwaves (highlighted in green in Table 4).

Table 4: Average annual number, air temperature and duration of heatwaves detected from each detection method.

Detection methods	Average annual number of heatwaves	Average air temperature	Average duration	Total number of heatwaves
Spic, Sdeb, Sint	1.89	28.3 °C	14.5 d	2384
IBMn, IBMx	1.77	30.3 °C	6.3 d	2229
EHF	6.06	24.8 °C	11.1 d	7641
HWMI	6.65	25.6 °C	6.9 d	8375

3.3. Step 3: Heatwave characterisation

3.3.1. Objectives and method

225 The third step of the methodology consists of defining the heatwave characterisation space. The heatwave characterisation space is a space for which each dimension corresponds to one heatwave indicator. Each heatwave indicator quantifies one characteristic of the heatwaves. Thus, the third step consists of establishing a list of relevant heatwave indicators.

230 [7] defined a heatwave characterisation space with three indicators: the duration, the maximum temperature and the severity (also named global intensity) of the heatwave. This three-dimensional characterisation space enables a graphical representation of a heatwave population, as shown in Figure 2. In this graph, the size of the bubbles indicates the global intensity of the heatwaves. The colour of the bubble depends on the year of the heatwave. This approach is limited: the three indicators are solely based on the evolution of the air temperature during the heatwaves. However, as mentioned in
 235 the introduction of the paper, the thermal behaviour of a building does not only result from the outside air temperature evolution. It also results from other weather parameters, such as solar radiation, sky temperature, wind speed, etc. A broader set of
 240 indicators based on those variables is needed to assess the diversity of heatwaves.

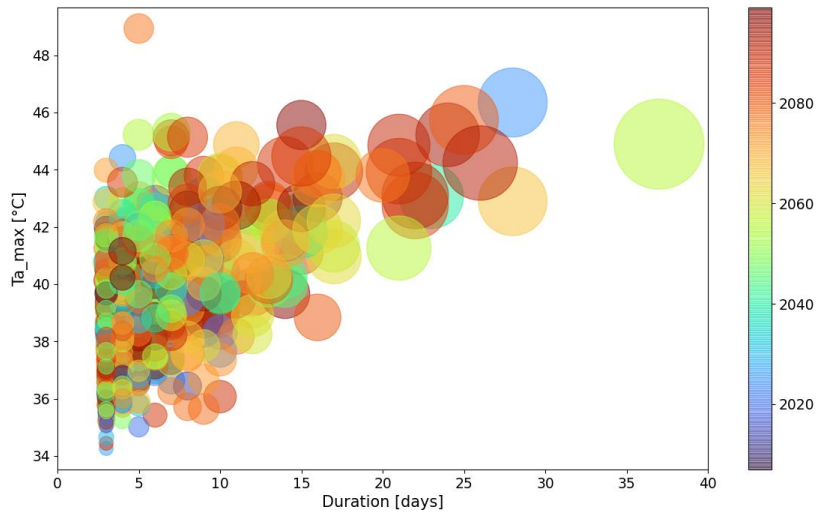


Figure 2: Heatwave characterisation space proposed by Ouzeau et al. (2016) for the heatwave detected with the “IBM” method for the RCP 4.5 scenario in the location of Lyon-Sain-Exupéry Airport. The weather predictions of all the models are mixed in this figure. The colour bar indicates the year of each heatwave. The size of the bubble represents the global intensity of the heatwave.

245

Given the amount of data that is available for each heatwave, there is almost an infinite number of possible heatwave indicators. To the authors’ knowledge, there was no other choice than starting the third step by the definition of an arbitrary list of indicators.

250

The arbitrary list of indicators proposed in the present study is composed of 3 groups. The first group of indicators contains the heatwave duration, the day of the year corresponding to the first day of the heatwave, and some basic statistics computed from the values of the different weather variables. The basic statistics are the average value (avg), the maximum value (max), the average value of the daily maximums, the daily minima (dmin_avg/dmax_avg) and the daily amplitudes (damp1_avg), the average value during the night-time and the day-time periods (nighttime/daytime), and the average value during the week before the heatwave occurs. Here, the night-time is fixed between 10 pm and 9 am, and the daytime is fixed between 10 am and 9 pm. It is not relevant to compute all those statistics for all the weather variables. Indeed, some

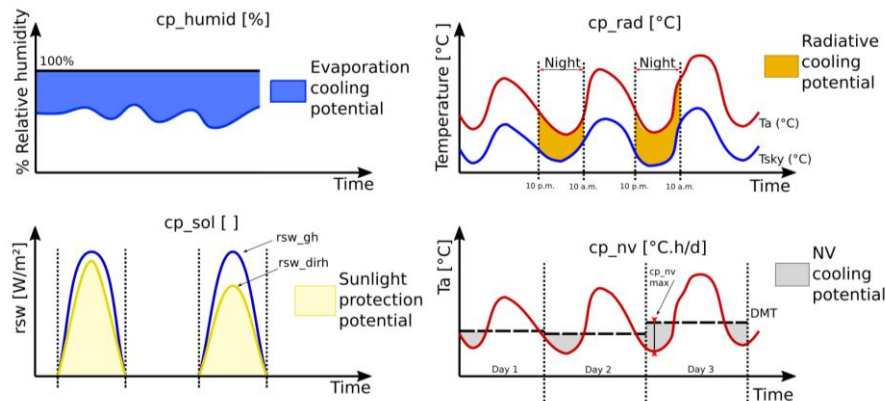
255

260 statistics would represent quantities that would not affect a building's thermal behaviour. Table 5 summarizes all the statistics computed for each weather variable.

Table 5: First group of the extended set of indicators, inventory of the statistics computed for each weather variable

Weather variable	avg	max	damp1_avg	dmin_avg/dmax_avg	nighttime/daytime
Dry air temperature [°C]	x	x	x	x	x
Specific humidity [kg/kg]	x				
Relative Humidity [%]	x				x
Sky temperature [°C]	x				x
Global horizontal radiation [W/m ²]	x				
Direct horizontal radiation [W/m ²]	x				
Cloud cover	x				
Wind speed [m/s]	x				x
Precipitation [kg/m ² /s]	x	x			

265 The second group of indicators is composed of cooling potential indicators. The cooling potential indicators quantify the opportunities offered by the weather conditions for a building to adopt passive cooling strategies. There are four “cooling potential” indicators for the four common passive bioclimatic strategies: radiative cooling (cp_rad), solar shading (cp_sol), evaporative cooling (cp_humid), and natural
 270 ventilation (cp_nv). Their definitions are represented schematically in Figure 3. The radiative cooling potential is the average value of the difference between the air temperature and the sky temperature during the nighttime periods. The solar shading cooling potential is the ratio between the total horizontal direct solar radiation (rsw_dirh) and the total global horizontal solar radiation (rsw_gh). The evaporating
 275 cooling potential is the average value difference between the relative humidity of saturated air (100%) and the relative humidity of the actual outdoor air. The natural ventilation cooling potential is the average positive difference between the daily mean air temperature (DMT) and the nighttime air temperature.



280 *Figure 3: Cooling potential (by evaporation top left, by direct radiation protection bottom left, by nighttime
heat radiation top right and by natural ventilation bottom right)*

The third group of indicators is composed of global intensity (or severity) indicators. Global intensity indicators were produced together with heatwave identification
285 methods. There are 3 heatwave intensity indicators: the intensity_spic defined by Ouzeau et al. (2016) associated with the “Spic, Sdeb, Sint” identification method, the intensity_ehf defined by Nairn et al. (2014) associated with the “EHF” identification method and the intensity_hwmi defined by Russo et al. (2014) and associated with the “HWMI” identification method.

290 The union of the three groups of indicators constitutes the initial extended list of 33 indicators.

With an initial extended list of indicators established, an analysis of the correlation between the indicators’ values for the whole heatwave dataset is performed. The correlation analysis aims to meet two objectives. The first objective is to reduce the
295 number of indicators by eliminating redundant ones. If the values of two indicators are strongly correlated, the way they differentiate heatwaves is similar, and there is no need to keep both indicators in the list. The second objective is to obtain information about the possible presence of trends in heatwave characteristics within the heatwave dataset. The number of independent indicators measures the level of independence between the
300 different heatwave characteristics. The higher this level of independence is, the higher

the number of heatwaves that would be needed to represent the diversity of the heatwave characteristics in the dataset.

A graphical method is proposed to conduct the correlation analysis. It consists of drawing an arranged correlation matrix and identifying groups of highly correlated indicators within the matrix. This is the correlation matrix analysis (CMA). An arranged correlation matrix is a correlation matrix for which the position of the indicators is arranged to put the indicators that are highly correlated closer to each other. The matrix of correlation is computed with the absolute value of the Pearson correlation. The position of the indicators in the matrix is arranged with a hierarchical clustering technique. A hierarchical clustering technique is a combination of a metric between individual elements and a linkage method. The metric between individual elements is the absolute value of Pearson's correlation. The present paper does not recommend any linkage method. The user is invited to test different methods and to select the method for which the resulting matrix allows the best visual identification of groups of highly correlated indicators. Once the groups of highly correlated indicators are identified, one indicator is retained within each group. The other indicators are removed from the list. They are redundant.

The number of indicators is then further reduced by removing insignificant indicators. These insignificant indicator values are sufficiently narrow, so that variations in their values may not lead to significant changes in building performance. The identification of the insignificant indicators is based on the graphical representation of the distributions of indicator values. It is up to the user's degree of experience in building thermal behaviour to determine which variable may be insignificant.

3.3.2. Application/illustration

The values of all the indicators were computed for all the heatwaves within the extended heatwave dataset. Different combinations of linkage methods (average, ward, single, complete, weighted, centroid, median) were tested to draw the arranged correlation matrix. All those combinations resulted in similar groups of highly correlated indicators. The arranged correlation matrix on Figure 4 was obtained with the "single" linkage method corresponding to the "neared neighbour" metric between groups.

After a visual inspection of the matrix, ten groups of highly correlated indicators were arbitrarily delimited. These groups are identified with thick line rectangles in Figure 4. Two indicators are not correlated with each other and thus form two groups of one indicator: wind direction and average air temperature one week before the heatwave.

There is no real need to compute several statistics for each weather variable because those statistics are redundant. Indeed, most of the groups contain all the statistics related to one or two weather variables. For convenience, each group of indicators is named according to one of its related weather variables. The names are displayed at the bottom of Figure 4.

The heatwave duration (“duration”) and the global intensity (or severity) indicators (“intensity_hwmi” and “intensity_spic”) belong to the same group. This reveals that the global intensity indicators mostly measure the duration of the heatwaves and slightly modulate this duration with the air temperature. In other words, using one of the intensity indicators to describe heatwaves would not provide much additional information on the different heatwave characteristics if both the duration and the average air temperature indicators are already used. This correlation is visible in Figure 2, where it is clear that all the heatwaves with the highest intensity (larger bubbles) correspond to the longest heatwaves (on the right side of the graph).

The low correlation between solar global irradiation and solar direct irradiation was at first unexpected. It reveals the two distinct mechanisms that affect solar radiation. Global solar irradiation is related to the period of the year at which heatwaves occur. It is at maximum when a heatwave occurs in June. It decreases when a heatwave occurs in late summer because the sun position is lower at that time. The amount of direct solar radiation seems to be more affected by the presence of clouds in the sky.

Each cooling potential indicator is based on one or two weather variables. The cooling potential indicators belong to the group of indicators related to one of their associated weather variables. The evaporative cooling potential (“cp_humid”) belongs to the relative humidity group. The solar shading cooling potential (“cp_sol”) is within the direct solar radiation group. The “cp_rad” indicator is highly correlated to the sky temperature group. However, it is also highly correlated with the humidity group. The correlation between the sky temperature group and the humidity group is explained by

Duration	duration	Days	3	16	X
Main wind direction	wd_main	°	-	-	
Average wind speed	ws_avg	m/s	1.83	4.37	X
Average horizontal global solar radiation	rsw_gh_avg	W/m ²	207.03	321.33	X
Cooling potential by solar protection	cp_sol	/	0.41	0.92	X
Average sky temperature	tsky_avg	°C	10.14	18.6	X
Average relative humidity	rh_avg	%	26.99	57.34	X
Average temperature before the heatwave	ta_avg_prior	°C	22.24	30.37	X

Figure 5 shows the distributions of the ten independent indicator values. The 5th and 95th percentiles are given in the last two columns of Table 6. Two insignificant indicators are identified: the maximum precipitation and the main wind direction.

The 95th percentile of the maximum precipitation values is 2.5 mm/h. According to Météo-France, precipitation can be considered light rain when its flow rate is below 3 mm/h. Thus, during heatwaves, the maximum precipitation is very low, and only very little effect of rain on building behaviour is expected.

The distribution of the main wind direction values reveals two major directions: from north to south and from south to north. These directions are opposite to each other. The wind direction mostly affects natural ventilation flow rates within cross-ventilated buildings. In most cases, the effect of the wind direction on the natural ventilation flow rate is nearly symmetrical according to the wind direction. Two opposite directions would result in a similar flow rate.

Heatwaves can therefore be characterised by a space composed of eight dimensions, which correspond to the eight significant indicators in Table 6.

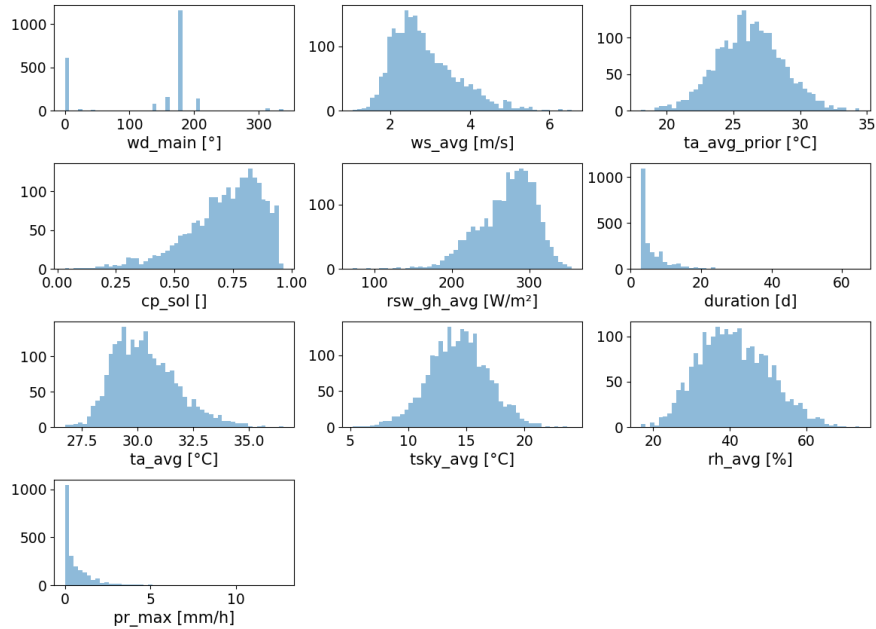


Figure 5: Histograms of independent indicator values among the extended heatwave dataset

395

3.3.3. Challenging the method with a principal component analysis

The identification of the independent indicators was performed with a correlation matrix analysis (CMA). Instead, this identification could have been performed with a principal component analysis (PCA). CMA involves arbitrary decisions from the user, such as the delimitation of the groups of indicators. PCA is a more rational technique, and it is less sensitive to user decisions. Performing a PCA on the extended indicator dataset and comparing the PCA results to the CMA results may allow us to assess the relevance of the CMA results.

The principal component of a dataset (PC) is the linear combination of variables for which the variance of the data is maximum. A PCA detects principal components iteratively in such a way that all the PCs are independent from each other (the correlation between the PC values is low). When detecting a new PC, the variance of the dataset that is explained by the list of PCs increases. The iterative process stops when this increase becomes negligible.

405

410 PCA was performed on the dataset containing the values of all the indicators for all
the heatwaves. The PCA provided a list of independent linear combinations of
indicators. This list can be compared to the list of independent indicators produced by
the CMA.

The PCA was run until 89% of the total variance of the dataset was explained by the
415 PCs. At this stage, eight PCs were selected. This confirms the high level of
independence between the indicators. The number of PCs (8) is comparable to the
number of independent indicators (10) selected with the CMA.

Table 7 reveals the three major contributors of the eight PCs. For almost all the PCs,
the three major contributors belong to the same group of independent indicators
420 identified with the CMA. The names of the corresponding groups are given in the last
column of the table. Each group appears only once. There is a direct link between the
PCs and the independent indicators. The PCA confirms the relevance of the CMA
results.

Table 7: Major contributors of the PCs

	1 st	2 nd	3 rd	Clustering group
PC1	ta_daytime	ta_avg	ta_dmax_avg	Air temperature
PC2	tsky_avg	tsky_nighttime	tsky_daytime	Sky temperature
PC3	ws_avg	ws_nighttime	ws_daytime	Wind
PC4	rsw_dirh_avg	day_of_year	rsw_gh_avg	Solar radiation
PC5	ta_damp1_avg	rsw_gh_avg	day_of_year	-
PC6	duration	intensity_hwmi	intensity_spic	Duration and intensities
PC7	pr_avg	pr_max	cp_sol	Rain
PC8	ta_avg_prior	wd_main	day_of_year	-

425

From the authors' point of view, the advantage of CMA, compared to PCA, is that
this technique allows a visual inspection of the heatwave dataset content and selects
indicators that are easier to interpret than principal components.

3.4. Step 4: Selecting heatwaves

430

3.4.1. Objectives and method

The sampling method presented in this section aims to construct a minimal representative set of heatwaves. The minimal representative set of heatwaves covers a maximum of the diversity of the heatwave characteristics, with a minimum number of heatwaves. The sampling method consists of grouping similar heatwaves with a clustering technique and then selecting a representative heatwave for each group. Those steps are performed in the heatwave characterisation space, with normalized indicator values along the dimensions.

The grouping process is ensured by a hierarchical clustering technique. It starts with all the heatwaves being in distinct clusters. At each iteration, the two closest clusters are merged. The metric between elements for the clustering technique is the Euclidian distance in the characterization space. The linkage method is the “Ward” linkage method. This linkage method aims at producing compact, spherical clusters by selecting the clusters to be merged based on an increase in the cluster Ward variances. The two clusters that are merged are the two clusters for which the increase in the combined variance over the sum of the cluster-specific variances is the minimum.

The distance between two clusters that have just been fused is called the dissimilarity distance. At the end of the linkage process, the cumulative dissimilarity distance is displayed as a function of the number of clusters. The optimal number of clusters is a compromise between a low number of clusters and a low dissimilarity distance. It is identified graphically with the elbow method, which is commonly used with the K-means clustering method [11].

Then, a representative heatwave is selected in each cluster. To do so, the distance D_k is computed for each heatwave of the cluster. The distance D_k is the sum of the Euclidean distances between the heatwave k and the barycentre of the other clusters:

$$D_k = \sum_{j \neq i} dist(k, barycenter(j)) \quad \forall k \in i$$

The representative heatwave of a cluster is defined as the heatwave corresponding to the 85th percentile of the distribution of D_k . This technique allows us to emphasise the dissimilarities between the different clusters and to cover a majority of the portion of the characterisation space occupied by the heatwaves without necessarily selecting outliers (Figure 6).

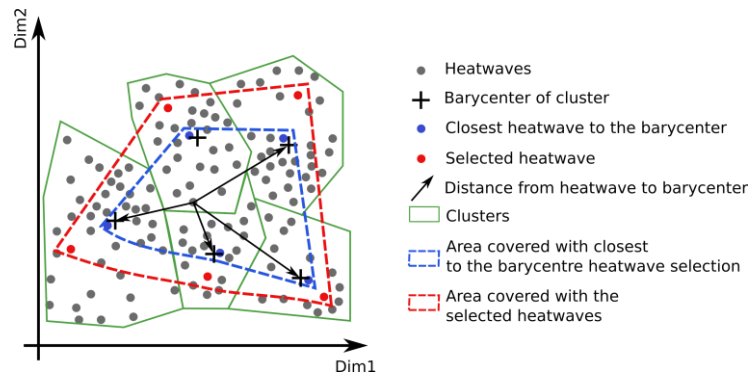
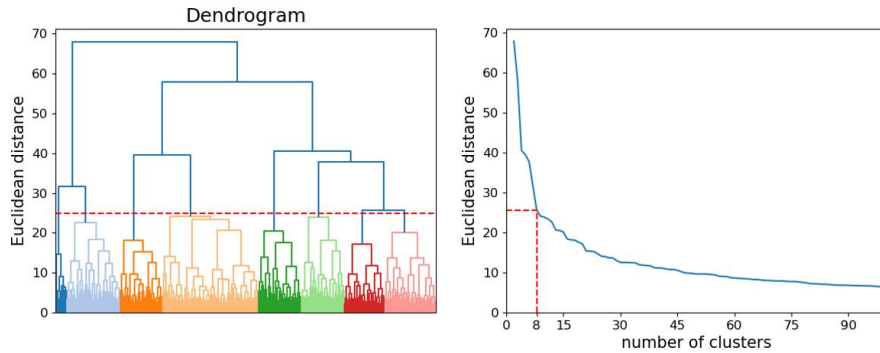


Figure 6: Representative heatwave selection and the space it covers on a 2D projection of the characterisation space.

3.4.2. Application/illustration

465 The result of the clustering process for Lyon-St Exupery is represented as a dendrogram in Figure 7 (left graph). In this graph, each junction between two branches represents the fusion between two clusters. The vertical distance between two consecutive junctions is the dissimilarity distance.

470 Figure 7 (right graph) shows the evolution of the dissimilarity distance as a function of the number of clusters. The curve is strictly decreasing: the higher the number of clusters is, the more similar the heatwaves are in each cluster. The elbow of the curve occurs when the number of clusters is equal to eight. Onwards, the decrease in the dissimilarity distance is strongly reduced. Choosing a larger number of clusters would not significantly reduce the distance between clusters, but it would considerably increase the number of simulations for assessing building performances. The last column of Table 8 shows the number of heatwaves in each cluster. The size of the clusters is well balanced. Each cluster contains between 240 and 560 heatwaves, except the last cluster, which contains 65 heatwaves.



480 *Figure 7: Dendrogram of the heatwave dataset in the characterisation space (left graph). Euclidean*
distance as a function of the number of clusters (right graph). The red dashed lines show the selected
number of clusters and the associated Euclidean distance.

One representative heatwave was selected within each cluster. Table 8 shows the values of the heatwave indicators for the eight representative heatwaves. A colour scale
 485 was applied to each column of the table to distinguish indicator values corresponding to lower stress (white colour) and indicator values corresponding to higher stress (red colour). The boundaries of the colour scales are the 5th and 95th percentiles of each indicator. Those quantiles are given in the third line of Table 8.

Each heatwave has a specific profile. The durations range between 3 days (short
 490 heatwave) and 30 days (exceptionally long heatwaves). The average air temperature oscillates between 28.8 °C and 34.3 °C. Some heatwaves have a lower average sky temperature (heatwaves 2 and 4) or a higher wind velocity value (heatwaves 2, 4 and 5), which may enhance passive cooling performance. Heatwaves 3 and 4 are the heatwaves for which the average air temperature during the preceding week is lower,
 495 enabling the building to store freshness before the beginning of the heatwave. Heatwaves 1, 2 and 7 occur around the summer solstice, when there is plenty of solar radiation. In contrast, heatwaves 4 and 5 occur late in the summer, when there is considerably less sun. Heatwaves 3 and 6 are significantly more humid than the other heatwaves. Heatwave 5 is much drier. Finally, the sky is clear during most heatwaves,
 500 resulting in over 70% of direct solar radiation, except for heatwaves 4 and 5, where the

proportion of direct radiation is 57% and 53%, respectively, and for heatwave 1, for which the direct solar radiation represents only 25% of the total solar radiation.

The eight heatwaves depict a wide variety of weather characteristics, which may result in a wide variety of building responses.

505

Table 8: Characteristics of the heatwaves contained in the minimum representative set of heatwaves

	duration	ta_avg	tsky_avg	ws_avg	ta_avg_prior	rsw_gh_avg	rh_avg	cp_sol	
Unit	[d]	[°C]	[°C]	[m/s]	[°C]	[W/m ²]	[%]	[-]	nb heatwaves
range	[3; 16]	[28.4; 33]	[10.1; 18.6]	[1.82; 4.37]	[22.2; 30.4]	[207; 321]	[27; 57.3]	[0.4; 0.9]	
1	3	31.16	17.68	3.65	25.18	307.88	41.4	0.25	
2	4	30.89	13.7	5.46	24.62	299.19	31.78	0.72	246
3	5	29.00	17.35	1.90	23.14	280.1	59.76	0.88	297
4	6	28.79	10.1	3.96	23.14	236.33	41.16	0.57	564
5	6	33.73	14.62	3.96	26.45	220.03	22.6	0.53	253
6	6	29.31	15.43	2.24	23.75	284.94	53.3	0.91	238
7	10	34.31	17.17	3.42	24.82	300.13	27.24	0.8	316
8	30	32.81	18.57	2.8	31.57	265.86	36.71	0.8	65

3.4.3. Validity of the clustering selection

The validity of the clustering selection is evaluated through a silhouette score analysis [12], as shown in Figure 8. The silhouette score $s(i)$ of a datapoint i lies between -1 and 1. When $s(i)$ is large (close to 1), the datapoint i is ‘well-clustered’; there is little doubt that i has been assigned to a very appropriate cluster. When $s(i)$ is low (near zero), it is not clear whether i should have been assigned to its cluster or to another cluster, and i lies equally far away from both, so it can be considered an ‘intermediate case’. The worst situation takes place when $s(i)$ is close to -1. In that case, it would have seemed much more natural to assign object i to another cluster. The object i has been ‘misclassified’ [12].

515

The mean value of the silhouette score for the heatwave clustering is 0.06 (red dashed vertical line in Figure 8). It is quite close to zero, which indicates that clusters are overlapping.

For Clusters 1, 3, 4, 5 and 7, half of the heatwaves are ‘well clustered’ with a positive silhouette score, and half of the heatwaves are ‘slightly misclassified’, with a negative silhouette score. For Clusters 2, 6 and 8, most of the heatwaves are ‘well clustered’.

520

Even if the silhouette score analysis reveals overlapping clusters, the representative heatwaves of each cluster seem to be quite different from each other, as represented in Table 8. It still allows a better representation of the meteorological diversity than using only one future heatwave.

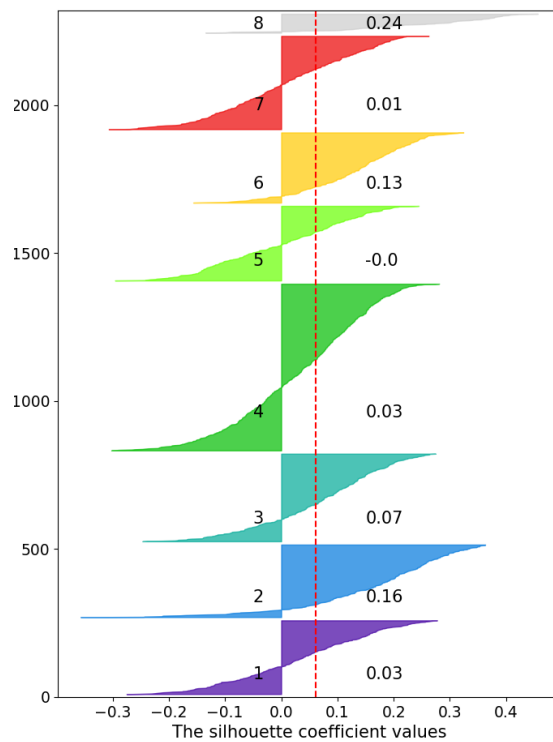


Figure 8: Silhouette score for each heatwave in the dataset. The red vertical dashed line indicates the mean of the silhouette score. The number on the right of each cluster indicates the mean value of the silhouette score for each cluster.

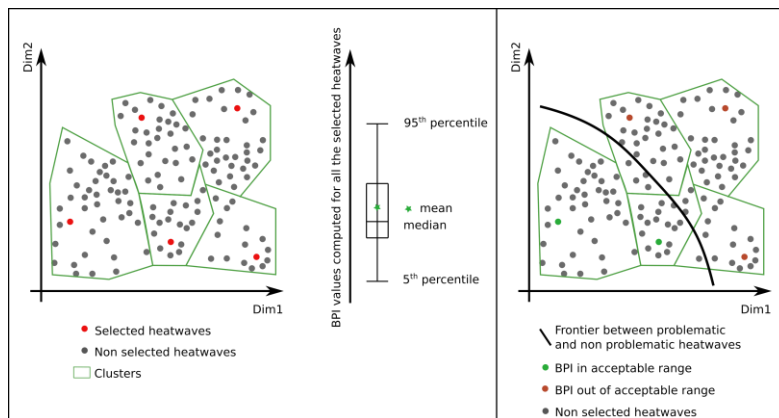
530 4. Usage and beyond

The minimum representative set of heatwaves should be the starting point of the evaluation of building performances under future heatwaves. Since the minimum representative set of heatwaves covers the whole diversity of future potential heatwave

characteristics, the simulations performed with this set of weather files may reproduce
535 the expected variety of building thermal behaviour during future heatwaves. Those
simulations may also produce a first population of building performance indicator
values (BPI) and allow us to have a first estimation of the amplitude of those values.

After performing those initial simulations, there are two ways to go deeper into the
investigation of future heatwave effects on buildings. These two methods are illustrated
540 graphically in Figure 9. The first method consists of sampling more heatwaves and
performing simulations until refined statistics of the BPI values can be computed
(average, standard deviation, etc.). The second usage would consist of refining the
localisation of the frontier between problematic and nonproblematic heatwaves in the
characterisation space. This usage would require establishing a BPI threshold to
545 distinguish problematic and nonproblematic heatwaves.

Both ways of going further into the investigation of future heatwave effects on
buildings would require a specific iterative algorithm to continue sampling heatwaves
in the characterisation space.



550 *Figure 9: Dispersion of a building performance indicator due to the variability of heatwaves (left graph)
and frontier between problematic and nonproblematic heatwaves in a 2-dimensional projection of the
characterisation space (right graph).*

5. Conclusions

555 The paper proposed a methodology for constructing a minimum representative set of future heatwave weather files dedicated to building performance evaluations. This methodology has been applied to the location of Lyon-St Exupery.

The set of heatwaves is representative in the sense that the heatwaves are sufficiently different from each other to cover the large spectrum of heatwave characteristics that a building could face in the location of Lyon-St Exupery. It is a minimum set; eight 560 heatwaves were proven to be sufficient to obtain a representative set of future heatwaves.

Building simulations should be performed with the minimum representative set of heatwaves to obtain an order of magnitude of the BPI dispersion during future heatwaves and to identify to which weather characteristics the building is the most 565 sensitive. Then, to obtain a more accurate description of the BPI value distribution or to refine the boundary between problematic and nonproblematic heatwaves, more weather files might be needed.

The minimum representative set of heatwave weather files might become an essential tool to evaluate building performance during future extreme events. It will 570 particularly be helpful for the most robust passive cooling strategies for the future.

6. Acknowledgements

We acknowledge the World Climate Research Program's Working Group on Regional Climate and the Working Group on Coupled Modelling, the former 575 coordinating body of CORDEX and the responsible panel for CMIP5. We also thank the climate modelling groups (listed in Table 3 of this paper) for producing and making available their model output. We also acknowledge the Earth System Grid Federation infrastructure, an international effort led by the U.S. Department of Energy's Program for Climate Model Diagnosis and Intercomparison, the European Network for Earth System Modelling and other partners in the Global Organisation for Earth System 580 Science Portals (GO-ESSP).

The authors gratefully acknowledge the Lyon Urban School (LUS) for funding this research work (ANR-17-CONV-0004).

7. References

- 585 [1] A. Machard, C. Inard, J.-M. Alessandrini, C. Pelé, et J. Ribéron, « A Methodology for Assembling Future Weather Files Including Heatwaves for Building Thermal Simulations from the European Coordinated Regional Downscaling Experiment (EURO-CORDEX) Climate Data », *Energies*, vol. 13, n° 13, p. 3424, juill. 2020, doi: 10.3390/en13133424.
- 590 [2] S. Ramakrishnan, X. Wang, J. Sanjayan, et J. Wilson, « Thermal performance of buildings integrated with phase change materials to reduce heat stress risks during extreme heatwave events », *Applied Energy*, vol. 194, p. 410-421, mai 2017, doi: 10.1016/j.apenergy.2016.04.084.
- [3] P. Lassandro et S. Di Turi, « Multi-criteria and multiscale assessment of building envelope response-ability to rising heat waves », *Sustainable Cities and Society*, vol. 51, p. 101755, nov. 2019, doi: 10.1016/j.scs.2019.101755.
- 595 [4] A. Laouadi, A. Gaur, M. A. Lacasse, M. Bartko, et M. Armstrong, « Development of reference summer weather years for analysis of overheating risk in buildings », *Journal of Building Performance Simulation*, vol. 13, n° 3, p. 301-319, mai 2020, doi: 10.1080/19401493.2020.1727954.
- 600 [5] O. Yaqubi, A. Rodler, S. Guernouti, et M. Musy, « Creation and application of future typical weather files in the evaluation of indoor overheating in free-floating buildings », *Building and Environment*, vol. 216, p. 109059, mai 2022, doi: 10.1016/j.buildenv.2022.109059.
- [6] S. E. Belcher, J. N. Hacker, et D. S. Powel, « Constructing design weather data for future climates », *Building Services Engineering Research and Technology*, 2005, doi: 10.1191/0143624405bt112oa.
- [7] G. Ouzeau, J.-M. Soubeyroux, M. Schneider, R. Vautard, et S. Planton, « Heat waves analysis over France in present and future climate: Application of a new method on the EURO-CORDEX ensemble », *Climate Services*, vol. 4, p. 1-12, déc. 2016, doi: 10.1016/j.cliser.2016.09.002.
- 610 [8] M. Pascal *et al.*, « France's heat health watch warning system », *Int J Biometeorol*, vol. 50, n° 3, p. 144-153, janv. 2006, doi: 10.1007/s00484-005-0003-x.
- [9] J. Nairn et R. Fawcett, « The Excess Heat Factor: A Metric for Heatwave Intensity and Its Use in Classifying Heatwave Severity », *IJERPH*, vol. 12, n° 1, p. 227-253, déc. 2014, doi: 10.3390/ijerph120100227.
- 615 [10] S. Russo *et al.*, « Magnitude of extreme heat waves in present climate and their projection in a warming world », *Journal of Geophysical Research: Atmospheres*, vol. 119, n° 22, Art. n° 22, 2014, doi: <https://doi.org/10.1002/2014JD022098>.
- 620 [11] D. J. Ketchen Jr. et C. L. Shook, « The application of cluster analysis in strategic management research: an analysis and critique », *Strat. Mgmt. J.*, vol. 17, n° 6, p.

441-458, juin 1996, doi: 10.1002/(SICI)1097-0266(199606)17:6<441::AID-SMJ819>3.0.CO;2-G.

- 625 [12] P. J. Rousseeuw, « Silhouettes: A graphical aid to the interpretation and validation of cluster analysis », *Journal of Computational and Applied Mathematics*, vol. 20, p. 53-65, nov. 1987, doi: 10.1016/0377-0427(87)90125-7.